

Iron-rich melts, magmatic magnetite, and superheated hydrothermal systems:
The El Laco deposit, Chile

Tornos et al.

Appendix DR1. Calculation of volume of fluid needed for a hydrothermal origin for the El Laco magnetite-apatite deposit.

The calculation of the amount of fluid needed to form a deposit of magnetite as massive El Laco with 1.5 Gt of magnetite ore has been calculated following the lever rule assuming the complete separation of an aqueous phase at 950°C from a crystallizing andesite originally having 3% wt H₂O (Stern et al., 1975; Burnham, 1979) and does not include significant amounts of water in hydrous magmatic minerals such as mica or amphibole that may also be present. The initial magmatic fluid is assumed to have a salinity of 7 wt% NaCl eq. (Heinrich et al., 2004) and it exsolves at low pressure in two immiscible high and low density aqueous fluids, respectively. The brine has between 40 and 60 wt% FeCl₂ as measured from Koděra et al. (2014) in brines separating from a diorite melt. Density of the andesite is assumed to be 2.8 g/cm³ and that of magnetite 5 g/cm³.

References cited

- Burnham, C. W., 1979, Magmas and hydrothermal systems, in Barnes, H. L., ed., *Geochemistry of Hydrothermal Ore Deposits*: New York, Wiley, p. 71-132.
- Heinrich, C. A., Driesner, T., Stefansson, A., and Seward, T. M., 2004, Magmatic vapor contraction and the transport of gold from the porphyry environment to epithermal ore deposits: *Geology*, v. 32, p. 761-764. doi: 10.1130/G20629.1.
- Koděra, P., Heinrich, C. A., Wälle, M., and Lexa, J., 2014, Magmatic salt melt and vapor: Extreme fluids forming porphyry gold deposits in shallow subvolcanic settings: *Geology*, v. 42, p. 495-498. doi: 10.1130/G35270.1.

Stern, C. R., Huang, W.-L., and Wyllie, P. J., 1975, Basalt-andesite-rhyolite-H₂O: Crystallization intervals with excess H₂O and H₂O-undersaturated liquidus surfaces to 35 kbs, with implications for magma genesis: Earth and Planetary Science Letters, v. 28, p. 189-196.
doi:10.1016/0012-821X(75)90226-5

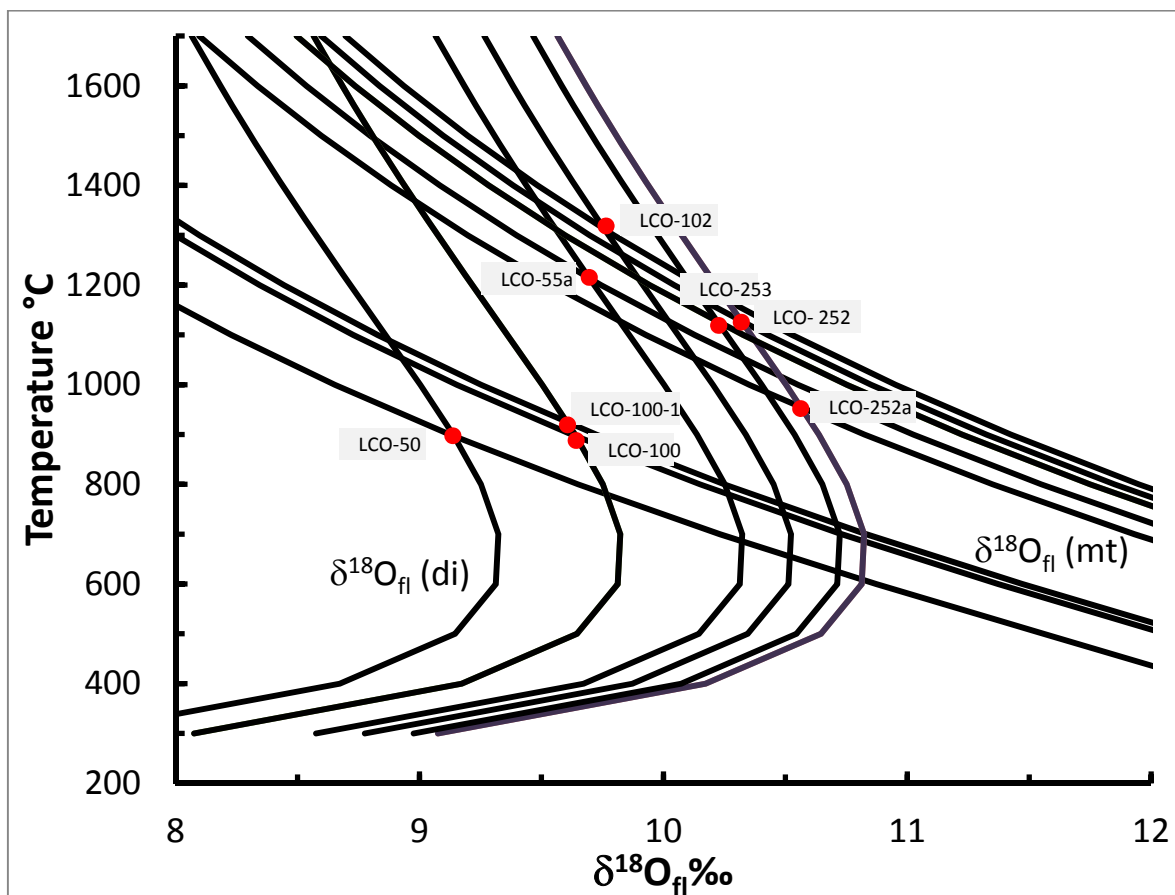


Figure DR1: Temperature vs calculated $\delta^{18}\text{O}_{\text{fluid}}$ for diopside-magnetite pairs estimated from the isotope values and the fractionation factors in Table DR1. The pairs give internally consistent temperatures despite the steep slope of the $\Delta_{\text{mt}-\text{H}_2\text{O}}$ and $\Delta_{\text{di}-\text{H}_2\text{O}}$ curves at high temperatures. Most estimated temperatures cluster around 900 and 1150 °C.

Table DR1. Stable isotope data for El Laco ores and related rocks.

Sample	Description	$\delta^{18}\text{O}_{\text{SMOW}} (\text{\textperthousand})$			$T^{\circ}\text{C} (\Delta_{\text{mt-di}})$
		Whole rock	Magnetite	Diopside	
LC-13	El Laco - pre-ore andesite	7.4			
LC-33	El Laco - post-ore andesite (plug)	8.4			
LC-34	El Laco - post-ore andesite (plug)	9.6			
LC-35	El Laco - post-ore andesite (plug)	7.5			
LC-36	El Laco - post-ore andesite	7.7			
LC-37	El Laco - post-ore andesite	8.7			
LC-38	El Laco - post-ore andesite	8.1			
LC-6	El Laco - massive magnetite stratabound ore			4.7	
LC-7	El Laco - massive magnetite stratabound ore			4.9	
LC-8	El Laco - massive magnetite stratabound ore			4.4	
LC-8a	El Laco - massive magnetite stratabound ore			4.4	
LC-8b	El Laco - massive magnetite stratabound ore			4.8	
LC-9	El Laco - massive magnetite stratabound ore			4.6	
LC-9a	El Laco - massive magnetite stratabound ore			4.8	
LC-9b	El Laco - massive magnetite stratabound ore			4.8	
LC-10	El Laco - massive magnetite stratabound ore			5.0	
LC-11	El Laco - massive magnetite stratabound ore			4.6	
LC-11a	El Laco - massive magnetite stratabound ore			4.6	
LC-24	El Laco - massive magnetite intergrown with apatite dykes			4.5	
LC-25	El Laco - massive magnetite intergrown with apatite dykes			4.5	
LC-26	El Laco - massive magnetite intergrown with apatite dykes			4.5	
LC-26b	El Laco - massive magnetite intergrown with apatite dykes			4.3	
LCO-50	Veins diopside-magnetite-anhydrite		4.4	7.2	897
LCO-55a	Veins diopside-magnetite-anhydrite		6.3	8.2	1213
LCO-56	Veins diopside-magnetite-anhydrite			8.1	
LCO-100	Veins diopside-magnetite-anhydrite		4.9	7.7	897
LCO-100-1	Veins diopside-magnetite-anhydrite		5.0	7.7	924
LCO-102	Veins diopside-magnetite-anhydrite		6.7	8.4	1312
LCO-105	Veins diopside-magnetite-anhydrite			7.8	
LCO-252	Veins diopside-magnetite-anhydrite		6.6	8.7	1126
LCO-252a	Veins diopside-magnetite-anhydrite		6.1	8.7	953
LCO-253	Veins diopside-magnetite-anhydrite - magnetite		6.5	8.6	1126

Notes: Analyses of stable isotopes were obtained at the Servicio General de Isótopos Estables, Universidad de Salamanca, Spain. Error is better than $\pm 0.1\text{\textperthousand}$ and the estimated temperature is $\pm 50^{\circ}\text{C}$. Fractionation factors from Zheng and Simon (1991) for magnetite (mt)-H₂O, Zheng (1993) for diopside (di)-H₂O and Zhao and Zheng (2003) for andesite-H₂O. Equilibrium temperature obtained from the comparison between the $\Delta_{\text{mt-H}_2\text{O}}$ and $\Delta_{\text{di-H}_2\text{O}}$.

Zhao, Z. F., and Zheng, Y. F., 2003, Calculation of oxygen isotope fractionation in magmatic rocks: Chemical Geology, v. 193, p. 59-80.

Zheng, Y. F., 1993, Calculation of oxygen isotope fractionation in anhydrous silicate minerals: Geochimica Cosmochimica Acta, v. 57, p. 1079-1091.

Zheng, Y.-F., and Simon, K., 1991, Oxygen isotope fractionation in hematite and magnetite: A theoretical calculation and application to geothermometry of metamorphic iron-formations: European Journal of Mineralogy, v. 3, p. 877-886.